

Huygens-Fresnel wavefront tracing in non-uniform media

F.A. Volpe, P.-D. Létourneau, A. Zhao

Dept of Applied Physics and Applied Mathematics, Columbia University, New York, NY

Abstract

We present preliminary results on a novel numerical method describing wave propagation in slowly non-uniform media. Following Huygens-Fresnel's principle, we model the wavefront as an array of point sources that emit wavelets, which interfere. We then identify a set of new points where the electric field has equal phase. In fact, without losing generality, we find zeros of the electric field, by means of the bisection method. This obviously corresponds to a specific phase-advance, but is easily generalized, e.g. by phase-shifting all sources. The points found form the new wavefront. One of the advantages of the method is that it includes diffraction. Two examples provided are diffraction around an obstacle and the finite waist of a focused Gaussian beam. Refraction is also successfully modeled, both in slowly-varying media as well as in the presence of discontinuities. The calculations were performed in two dimensions, but can be easily extended to three dimensions. We also discuss the extension to anisotropic, birefringent, absorbing media.

Keywords: Huygens-Fresnel principle, wavefront tracing, ray tracing, full wave, computational electromagnetism, diffraction

PACS: 42.15.Dp, 42.25.Bs, 42.25.Fx, 42.25.Gy, 42.25.Lc

1. Introduction

Huygens stated in 1690 that “each element of a wavefront may be regarded as the centre of a secondary disturbance which gives rise to spherical wavelets”. He added that “the position of the wavefront at any later time is

Email address: fvolpe@columbia.edu (F.A. Volpe)

the envelope of all such wavelets” [1, 2]. This result is referred to as Huygens’ theorem or construction. Indeed we can use it to construct subsequent wavefronts, if we ascertain some subtleties in what “envelope” means in this context. Such subtleties were eventually addressed by Fresnel [3, 4, 5], as discussed below. Also, the construction should be regarded as a mathematical abstraction that correctly reproduces the physics without necessarily being physically rigorous. Treating the wavefront elements as actual centers of secondary disturbances might be appropriate in some physics areas, but should not be taken literally in optics: obviously “light does not emit light; only accelerating charges emit light” [6], and the construction should be put in the context of what was known and understood in 1690. Yet, a principle of equivalence guarantees the validity of Huygens’ results: given two adjacent domains, 1 and 2, and given a wave in domain 1 approaching domain 2, it is possible to define conditions at the boundary between 1 and 2 (charges oscillating at the proper frequency, amplitude and direction) such that the wave excited in domain 2 by these boundary sources is indistinguishable from the wave entering from domain 1. Note that the charges in question oscillate as if responding to the wave in domain 1. The only imperfection in Huygens construction is that it pictured point-emitters, whereas elementary dipoles are more appropriate, as discussed in Ref.[7] and in Sec.2.

In 1816 Fresnel postulated that Huygens’ secondary wavelets interfere with each other [3, 4]. At this point, we can look at the interference pattern, and identify the next wavefront as the locus of points with the same phase.

The combination of Huygens’ construction with the principle of interference is called Huygens-Fresnel principle [2] or, often, simply Huygens’ principle, and is an important principle in the theory of diffraction.

Hence, not surprisingly, the principle has been used for didactic physics widgets illustrating diffraction around an obstacle, diffraction through one or more slits [8], and the diffraction of a Gaussian beam (namely, its finite waist). The principle also accounts for refraction, provided wavelets expand with different velocities in different media, in inverse proportion with the respective indices of refraction. For this reason, Huygens’ principle has also been applied to Snell’s law [9].

Recently Huygens’ principle was also invoked in the design of metamaterials with new beam shaping, steering and focusing capabilities [10].

In addition, the Huygens’ construction and Huygens-Fresnel’s principle inspired numerical methods, briefly reviewed in the next two subsections. This is also not surprising, on considering that Huygens’ original drawings

[1] basically outlined an iterative graphical solver, vaguely reminiscent of a modern iterative solver on a computer.

1.1. Seismic wavefront tracing methods

Huygens' principle was considered in Ref.[11], but discarded due to the lack of physics rigor mentioned above [6].

Wavefronts are “traced” or “tracked” in seismology on the basis of ray-tracing results or of geometrical-optics-approximated calculations of shortest travel-time to points on a grid [12], which in optics is equivalent to Fermat's principle of least time. In particular, among grid-based methods, fast marching methods [13] and some earlier works [14] are close to Huygens' idea, in that they treat the wavefront as a moving interface. Ray tracing ignores diffraction by definition, but calculations of shortest travel-time interrogate all points in a domain, including points around an obstacle. This might look promising for the inclusion of diffraction effects. Yet, it should be pointed out that these methods typically solve the Wentzel-Kramers-Brillouin (WKB) approximated eikonal equation. Therefore, the wave field is only accurate in the high-frequency, short-wavelength limit.

An interesting and elegant method is developed in Refs.[15, 16]. Again, the starting point is the eikonal equation, but manipulated into the expression:

$$[x - x(\gamma, \phi)]^2 + [y - y(\gamma, \phi)]^2 + [z - z(\gamma, \phi)]^2 = r^2(\gamma, \phi), \quad (1)$$

where γ and ϕ are curvilinear coordinates on the wavefront, $x(\gamma, \phi)$, $y(\gamma, \phi)$, $z(\gamma, \phi)$ are the Cartesian coordinates of a (source) point on the wavefront, and x, y, z the coordinates of another point, which can be pictured as a receiver. Eq.1 describes a sphere centered at $x(\gamma, \phi), y(\gamma, \phi), z(\gamma, \phi)$, of radius $r(\gamma, \phi) = v(\gamma, \phi)\tau$, where v is a velocity. As time τ progresses, the sphere expands. Differentiating Eq.1 eventually leads to an explicit finite-difference scheme: the coordinates of a point on the new wavefront are functions of the local r and of the coordinates of some points on the current wavefront. In particular, stencils of three and five points are used respectively in the 2D and 3D problem. The analogies with Huygens' construction are evident. However, Eq.1 contains no information on the strength of individual point-sources. Also, each new point is only informed by three or five points in its vicinity, whereas diffraction integrals imply that every point on the new wavefront depends on every point on the old one. Hence, although the numerical technique is highly stable [15, 16], small phase-increments might be

required in between consecutive wavefronts, in order for the restriction to three or five points to be a good approximation.

1.2. Other wavefront tracing and Huygens-related methods

Transmission Line Matrix Modeling [17] maps the problem of wave propagation in a medium into the problem of electrical signal propagation in a 3D array of shunt and series nodes. It can be shown that this is equivalent to Huygens' mechanical model of light as a perturbation of the Ether, originated by intense heat and transmitted by elastic shocks from one particle to the next, in all directions [17]. It is also equivalent to a many-body scattering problem, in which each node scatters light emitted by other nodes. It is possible to include diffraction by proper formulation of the scattered wave, or by adding *ad hoc* dielectrics to the array mentioned above [18].

Face offsetting [19] is a Lagrangian algorithm that treats an interface as a surface-mesh, propagates the mesh faces and, from their envelope, reconstructs the next surface, and its vertices. The method is based on a generalization of Huygens' original construction and envelope idea, but without Fresnel's addition of wavelet-interference.

Diffraction by rough surfaces (thus, ultimately, Huygens-Fresnel principle) is the physical explanation for iridescent colors. However, their rendering in computer graphics is simply obtained by angle-dependent coloration of surfaces in ray tracings [20].

Recent algorithms [21] utilize the Huygens-Kirchhoff integral to integrate many locally valid asymptotic Green functions into a globally valid asymptotic Green function for the Helmholtz equation in inhomogeneous media. However, they are formulated under geometrical optics approximations.

Additional methods and potential numerical applications of Huygens' principle are discussed in Ref.[22].

Note that "wavefront tracing" here refers to reconstructing several wavefronts in a propagation problem, whereas "wavefront reconstruction" in large telescopes denotes the inverse problem (phase retrieval) of reconstructing, from sensor measurements, a single incoming wavefront, in order to decide how to make it planar by means of adaptive optics [23]. Yet, there might be synergies with the method proposed here, one step of which is indeed phase retrieval (Sec.2.3). Wavefront reconstruction includes diffraction.

1.3. Present work

In summary, although several numerical works use Huygens construction of emitters and wavelets, few of them utilize the Huygens-Fresnel principle in its entirety, including wavelet interference (that is, diffraction).

A very simple numerical method is presented in Sec.2 of the present article, that retains more than 3 or 5 points in the diffraction integrals, takes into account their different intensities and utilizes a zero-search to localize the points forming the new wavefront. Sec.3 presents numerical examples obtained in a 2D isotropic non-uniform medium.

The original motivation for this work stemmed from the search for wave propagation methods in magnetized plasmas, intermediate in physics content and computational cost between ray-tracing [24, 25, 26] and beam-tracing or paraxial Wentzel-Kramers-Brillouin (WKB) methods [27, 28] on one hand, and full-wave solvers [29, 30] on the other. In turn, such need was prompted by unexpected results from the first full-wave study in the electron cyclotron frequency range [31] -a high-frequency range, typically well-modeled by ray tracings. However, the method proposed here is not restricted to magnetized plasmas, and could be extended to generic 3D anisotropic birefringent media, as discussed in Sec.5.

2. Numerical Method

2.1. Governing equation

Consider a wave in a medium, of wavenumber $k = 2\pi/\lambda$, where λ is the wavelength in the medium. In general, k and λ differ from the wavenumber and wavelength in vacuum.

The Huygens-Fresnel formula for the complex field amplitude \mathbf{E} in a point \mathbf{x}' can be written as follows [32]:

$$\mathbf{E}(\mathbf{x}') = \frac{1}{4\pi} \int_S \left[\frac{\cos \theta}{r} - ik(1 + \cos \theta) \right] \frac{e^{ikr}}{r} \mathbf{E}(\mathbf{x}) dS, \quad (2)$$

where \mathbf{x} is the generic point on surface S , representing the initial wavefront. θ denotes the angle between the local wavefront-normal and the vector $\mathbf{x}'-\mathbf{x}$, of norm r .

Strictly speaking, Eq.2 is only correct for uniform media, which, however, can often also be treated analytically. Nonetheless, it is not unusual and perhaps more useful and interesting to also use Eq.2 [33, 34, 35, 36, 37] or

other Huygens-based expressions [12, 15, 16, 21, 38] in weakly non-uniform media (in the sense that these media can be treated as locally uniform on the lengthscale of a single numerical step, but could have different refractive properties in the following step, and the wave have a different k and λ as a result).

Said otherwise, the formula is still applicable if the steplength is properly chosen, so that \mathbf{x}' is “not too far” from any \mathbf{x} , in the sense that $L = \left(\frac{1}{k} \frac{dk}{dx}\right)^{-1} \gg |\mathbf{x}' - \mathbf{x}|$. Here L is the lengthscale over which the medium (hence, the wavenumber k) varies. Note that the constraint on \mathbf{x}' not being too far depends on L . Also note that the approximation does not necessarily depend on how L compares with the wavelength $\lambda = 2\pi/k$. In other words, even if the medium varies significantly over a wavelength λ , Eq.2 can still be used to calculate \mathbf{E} in a point \mathbf{x}' close enough to S (“close enough” in the sense that the medium is practically uniform over that short distance). In fact, any ordering of the wavelength λ with respect to L and $|\mathbf{x}' - \mathbf{x}|$ is acceptable: greater than both, smaller than both, or intermediate.

In 2D, the surface integral is replaced by a line integral, and the denominator by \sqrt{r} , because the intensity of a cylindrical wave decays like $1/r$ [21, 39]:

$$\mathbf{E}(\mathbf{x}') = e^{-i\pi/4} \int_l \sqrt{\frac{1 + \cos \theta}{2\lambda}} \frac{e^{ikr}}{\sqrt{r}} \mathbf{E}(\mathbf{x}) dl. \quad (3)$$

The integrand is more complicated than expected from Huygens’ simplistic point sources. To begin with, the elementary sources emit with different intensities in different directions. This was conjectured by Fresnel to reconcile theory and experiment, and was rigorously calculated by Stokes [2]. It responds to the intuition that, given a source and two observers, one with a direct line of view, the other located around a corner, the former should receive more light.

Another correction is the $\cos \theta/r$ term in Eq.2. This is needed to make Huygens-Formula valid also in the near-field, and consistent with the more general and rigorous Kirchhoff integral theorem [7]. Its physical meaning is that the elementary sources should actually be radiating dipoles.

Indeed, dipoles are routinely used in modeling meta-lenses, frequency-selective surfaces and other diffraction-based devices [40, 41, 42].

Note that Eqs.2 and 3 are *not* equations to solve. They are rather *solutions*, in 3D and 2D, of the Helmholtz equation governing electromagnetic wave propagation in uniform (and, with some approximation, *slowly* non-

uniform) media. With special care, they can also describe propagation in strongly non-uniform media (see Figs.3 and 4 and accompanying discussion).

These solutions are constructed as superpositions of point-to-point solutions, propagating from a point-emitter to a point-observer. The treatment presented in the present paper permits to efficiently calculate integrals 2 or 3 in realistic domains with obstacles and non-uniformities. Its outcome are wavefronts reconstructed with high precision -strongly sub-wavelength. Yet, these finely reconstructed wavefronts can be sought at large distances from each other (large compared with the wavelength, but small compared with the lengthscale of inhomogeneity).

The treatment presented is easily generalized to other problems, provided the point-to-point propagator (Green's function) is known, and the superposition principle is valid.

2.2. Wavefront construction by zero localization

Given a wavefront S , our objective is to compute the integral in Eq.2 to identify a set of points \mathbf{x}'_{ab} (with $a=1, \dots, m$ and $b=1, \dots, n$) where \mathbf{E} has equal phase. Without losing generality, we can search for $\Re(\mathbf{E})=0$: if $\mathbf{E} = \mathbf{A}e^{\phi}$, then $\Re(\mathbf{E})=0$ implies either zero amplitude ($\mathbf{A} = \mathbf{0}$) or a specific phase ($\cos \phi=0$). However, the trivial solution of zero amplitude is easily rejected: zero amplitude means no wave, and if there is no wave in \mathbf{x}' , presumably there is no wave in a neighborhood of \mathbf{x}' . By contrast, $\Re(\mathbf{E})=0$ as due to $\cos \phi=0$ can only be true on a particular wavefront.

This search for a specific phase ($\phi = \pi/2$ modulo π) is easily generalized to a different phase by shifting all sources in the integrand by a certain $\delta\phi$. The points found form the new wavefront.

Equivalently, one could search for the locus of points where the phase of the total electric field, $\arctan[\Im(\mathbf{E})/\Re(\mathbf{E})]$ equals the phase of interest, ϕ . This can also be casted as a zero-search problem.

The existence of multiple solutions is prevented by restricting the search to intervals of length $\lambda/2$, where λ is the wavelength in the medium. It should be clarified that the *length* of the search-interval has nothing to do with its *positioning*: the search-interval can be placed close to the wavefront S or far from it, depending on the desired resolution (in the sense of inter-wavefront spacing) and on the validity of Eq.2 at that distance from S (in other words, is it still $|\mathbf{x}' - \mathbf{x}| \ll \left[\frac{1}{k} \frac{dk}{dx}(\mathbf{x})\right]^{-1}$ for any \mathbf{x}' on the $\lambda/2$ long search-interval and for every \mathbf{x} on surface S ?). Note that the wavefront-to-wavefront distance depends on the positioning of the search-intervals, not on their length. An

important consequence is that acceptable wavefront-to-wavefront distances (thus, computational costs) do not depend on λ ; they only depend on the inhomogeneity of the medium.

Depending on where the user places the search-intervals, the algorithm will trace the wavefront at phase $\phi = \pi/2$, or $3\pi/2$, or $5\pi/2$ etc. from the current one. As discussed, this is because sources have zero initial phase in Eq.2. Nonetheless, different wavefront-to-wavefront phase-increments (different from odd multiples of $\pi/2$) can also be obtained. For this purpose we can perturb the phase at the sources ($e^{ikr}\mathbf{E}(\mathbf{x}) \rightarrow e^{ikr+i\phi}\mathbf{E}(\mathbf{x})$) while still searching for zeros at the receivers ($\Re[\mathbf{E}(\mathbf{x}')] = 0$).

At least two approaches can now be envisioned for either zero search (that is, of $\Re(\mathbf{E})$ or $\arctan[\Im(\mathbf{E})/\Re(\mathbf{E})] - \phi$).

A possible approach is to locally solve Maxwell’s equations in such volume, in presence of point-sources located on the current wavefront. Computational electromagnetics methods, including but not limited to finite differences and finite elements, could repetitively solve the “local” problem in front of the present wavefront. However, in general this approach offers no major advantage compared to solving the problem once in the “global” domain. The approach is only advantageous if the union of the local domains is smaller than the global domain.

More interestingly, and more in line with the spirit of the Huygens-Fresnel principle, we can let the original point-sources interfere and we can localize iso-phase points to construct the new wavefront. In particular, we can look for loci of destructive interference (zeros).

2.3. Varying the phase-step

The zero-search is conducted on a $\lambda/2$ long segment. Depending on the positioning of the search intervals, different zeros could be found, corresponding to a different wavefront or, which is the same, to a different phase-advance $\Delta\phi$ (modulo π) with respect to the previous front. It is necessary to consistently place the search-intervals in such a way that they bracket zeros all belonging to the same wavefront. In other words, the search intervals need to “bracket” the unknown wavefront with a precision of $\lambda/2$.

This provides a simple knob to vary the phase-advance from one wavefront to the next: it is sufficient to consistently move all search-intervals farther from or closer to the current wavefront to vary the phase-advance by $n\pi$, where n is an integer.

For finer adjustments of ϕ , one can use complex \mathbf{E} in the integrand of Eq.2 or, equivalently, multiply the integrand by $e^{i\phi}$, which is equivalent to phase-shifting the sources.

2.4. Amplitude calculation and initialization of following iteration

If the wavefront was constructed as a locus of zeros ($\Re(\mathbf{E})=0$), it would be unclear what the wave amplitude \mathbf{E} is in each point. This information is needed because the final wavefront of a given step is the initial wavefront for the following one, and its points need to be properly initialized with the correct amplitude.

For this, it will be necessary to either compute $\Im(\mathbf{E})$ in the wavefront points (if $\Re(\mathbf{E})$ is already known), or re-compute $\Re(\mathbf{E})$ in those same points, but with all sources phase-shifted by $\phi \neq n\pi$. Note that the wavefront points have already been identified and do not need to be identified again.

Also note that this helps discarding “false zeros” of the wave-field. By this we mean that, in addition to zeros ($\Re(\mathbf{E}) \simeq 0$) of the oscillating, non-negligible wave-field ($|\mathbf{E}| \neq 0$), there could be trivial zeros where $\Re(\mathbf{E}) \simeq 0$ and $|\mathbf{E}| \simeq 0$. Such zeros are located away from the wave beam, and are not relevant to wavefront identification.

2.5. Algorithm

The algorithm -in 2D to fix the ideas, in Cartesian coordinates x and y , but easily generalized to 3D- can be recapitulated and illustrated as follows.

Step 1: Discretize the current wavefront as a 1D array of points \mathbf{x}_a ($a=1, \dots, m$) emitting different intensities \mathbf{E}_a (color-coded in Fig.1a), distributed according to the beam-pattern.

The very first array can be at the antenna, phased array or last mirror and can have complicated shape or phase-pattern.

Step 2: Define $\lambda/2$ long search-intervals for the points \mathbf{x}'_A ($A=1, \dots, m$) that will form the next wavefront.

For simplicity they can have the same coordinates y as the previous points \mathbf{x}_a , and only span x (Fig.1b). In fact, they can be obtained by displacing all points \mathbf{x}_a by the same amounts Δx and $\Delta x + \lambda/2$. Avoiding to place such intervals too closely ($\Delta x \ll \lambda$) to the original wavefront will allow discarding the dipole correction.

Step 3: For A going from 1 to m :

- a) Consider the search-interval for \mathbf{x}'_A .

- b) Evaluate the field \mathbf{E}_{Ac} in a point \mathbf{x}'_{Ac} on that interval, where c denotes an iteration index in the zero-search, e.g. by bisection [43]. Note that \mathbf{E}_{Ac} (of fixed A) is obtained by interference of all point-sources ($a=1, \dots, m$) in Fig.1c, each one of amplitude \mathbf{E}_a , at distance $r_{Aa,c}$ from the target and inclination $\theta_{Aa,c}$:

$$\mathbf{E}_{Ac} = e^{-i\pi/4} \sum_{a=1}^m \sqrt{\frac{1 + \cos \theta_{Aa,c}}{2\lambda}} \frac{e^{ikr_{Aa,c}}}{\sqrt{r_{Aa,c}}} \mathbf{E}_a \Delta l_a \quad (4)$$

This is a discretization of Eq.3. In its present form, the number of field calculations in m observers due to m emitters scales like m^2 . However, unequally spaced Fast Fourier Transform methods [44] could make it scale like $m \log m$. Additionally, Eq.4 can be restricted to values of a (typically in the neighborhood of A) yielding non-negligible contributions (dashed lines in Fig.1c).

- c) Repeat step b) for various \mathbf{x}'_{Ac} “suggested” by the zero-finder in its convergence to the zero. Repeat until $|\Re(\mathbf{E}_{Ac})| < \epsilon$, where ϵ is a prescribed tolerance.
- d) Set point \mathbf{x}'_A equal to last \mathbf{x}'_{Ac} .
- e) Set field-amplitude in \mathbf{x}'_A equal to last $\Im(\mathbf{E}_{Ac})$ (Fig.1d).

Step 4: Repeat steps 1-3 until absorption, or until exiting from computational domain, or until other criterion is met. Use the final points and amplitudes of step 3 as initial points and amplitudes for step 1.

The 2D algorithm is easily generalized to 3D by adding a subscript b and summing and looping over it. Eq.4 needs to be replaced by:

$$\mathbf{E}_{ABc} = - \sum_{b=1}^n \sum_{a=1}^m \frac{ik}{4\pi} (1 + \cos \theta_{AB,ab,c}) \frac{e^{ikr_{AB,ab,c}}}{r_{AB,ab,c}} \mathbf{E}_{ab} \Delta S_{ab}. \quad (5)$$

3. Numerical examples

The first test consisted of aiming a plane wave in the x direction, with periodic boundary conditions in y , effectively simulating an infinitely wide planar wavefront. This very simple test worked as expected: the wavefront

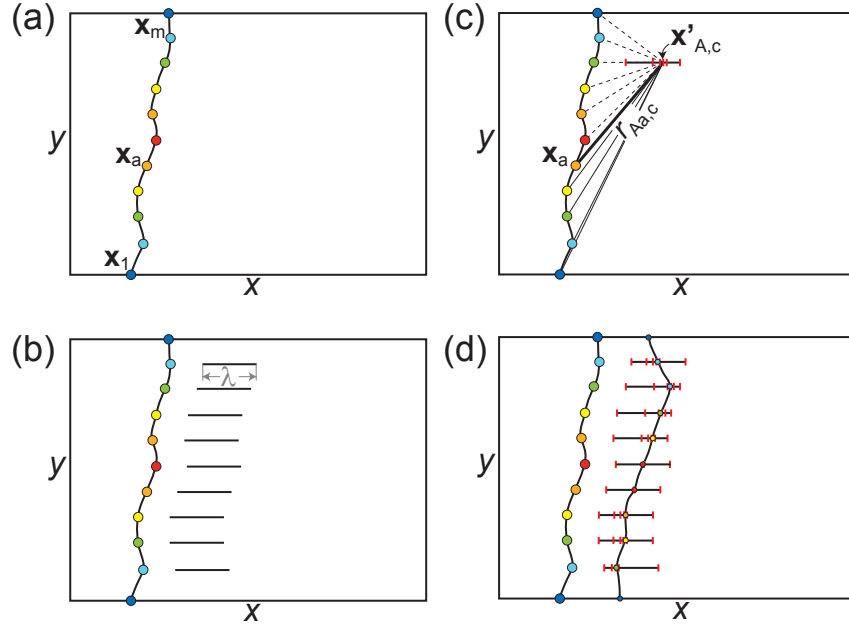


Figure 1: Illustration of (a) step 1, (b) step 2 and (c-d) step 3 of the algorithm described in Sec.2.5, for tracing a new wavefront based on the current one.

propagated in the x direction and remained planar (Fig.2a). This is in obvious agreement with the trivial analytical solution.

Next, an obstacle was placed at the bottom left of the computational box (Fig.2b). No periodic boundary conditions were used here, but additional emitters (“ghost cells”) were added at large y , outside of the computational box of interest. These acted as point-sources, which were taken into account in localizing new zeros and constructing new wavefronts, as well as calculating the amplitudes in wavefront points, for proper initialization of each step. Fig.2 clearly exhibits diffraction around the obstacle, as expected. At shallow angles past the obstacle, as expected, the wave field is weak and its zeros are not shown.

The next problem modeled was refraction in a non-uniform medium whose index of refraction varies slowly with space (ten wavelengths, in the case of Fig.3). The wavefront is planar, oblique. It extends outside of the computational domain by means of ghost cells on its top and bottom. As expected, the wavefront changes its direction of propagation according to the index of

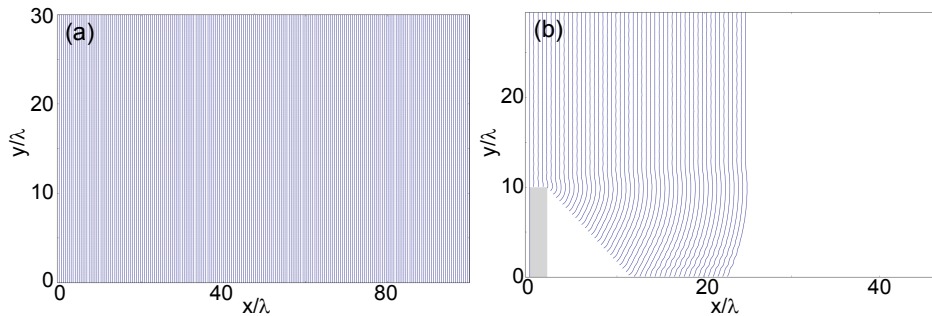


Figure 2: (a) Simple test of tracing planar wavefronts in uniform medium, in the absence of obstacles. (b) Initially planar wavefronts diffract around obstacle as expected.

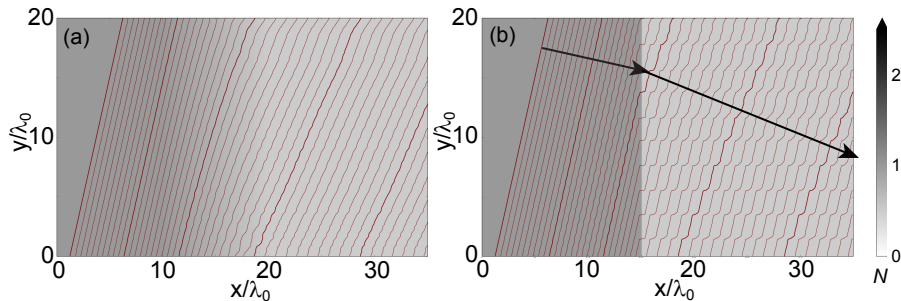


Figure 3: Wavefronts refracting in a medium of (a) refractive index N varying over ten wavelengths or (b) discontinuous.

refraction, in agreement with the continuous limit of Snell's law. The wavelength also contracts or expands accordingly, as it can be recognized from the wavefront spacing.

Discontinuities in the refractive index require special care. The reason is that the generic wavefront crossing a discontinuity has some points in medium 1, and some in medium 2. If \mathbf{E} is being evaluated in a point in medium 2, the contributions from points in medium 1 will travel initially at speed c/N_1 and then, once reached medium 2, at speed c/N_2 , where N_1 and N_2 are the refractive indices in the two media. Due to the principle of least time, the information does not travel on a straight line, but on two consecutive segments of different inclinations, obeying Snell's law. Therefore, instead of a single Green's function relating emitter i with observation point

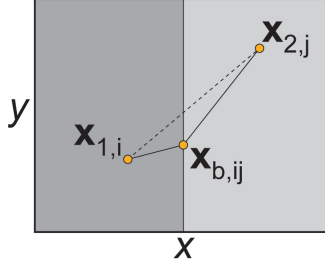


Figure 4: Illustration of why, in presence of discontinuities, a single Green’s function cannot propagate the information from an emitter in medium 1 to a receiver in medium 2, and an intermediate point is needed at the boundary, determined by Snell’s law.

j ,

$$\frac{e^{i\mathbf{k}\cdot(\mathbf{x}_j-\mathbf{x}_i)}}{|\mathbf{x}_j-\mathbf{x}_i|}, \quad (6)$$

we should introduce an intermediate point $\mathbf{x}_{b,ij}$ at the boundary, and use two propagators, from $\mathbf{x}_{1,i}$ in medium 1 to $\mathbf{x}_{b,ij}$, and then from $\mathbf{x}_{b,ij}$ to $\mathbf{x}_{2,j}$ in medium 2:

$$\frac{e^{i\mathbf{k}_2\cdot(\mathbf{x}_{2,j}-\mathbf{x}_{b,ij})}}{|\mathbf{x}_{2,j}-\mathbf{x}_{b,ij}|} \frac{e^{i\mathbf{k}_1\cdot(\mathbf{x}_{b,ij}-\mathbf{x}_{1,i})}}{|\mathbf{x}_{b,ij}-\mathbf{x}_{1,i}|} \quad (7)$$

For a given pair of $\mathbf{x}_{1,i}$ and $\mathbf{x}_{2,j}$, $\mathbf{x}_{b,ij}$ is uniquely determined by Snell’s law (Fig.4).

The wavefront bends as expected from Snell’s law (Fig.3b), in agreement with the analytical result. Corrugations similar to Fig.3a, but stronger, are ascribed to a lack of ghost cells, and will be the subject of future work. The construction of search-intervals will also be improved, by better bracketing of the zeros of interest.

Related to refraction by a single discontinuity is refraction by two consecutive ones. Wavefronts experience this when crossing a lens, and are observed to deform as expected, for example in the case of a convergent lens of refractive index $N=1.2$ (Fig.5).

Propagation through a single lens can be easily generalized to propagation through a random medium consisting of variously shaped “blobs” or grains immersed in a background material of different refractive index.

Finally, a Gaussian beam was simulated. Point-emitters were initialized on an initial curved wavefront, with intensities distributed according to a

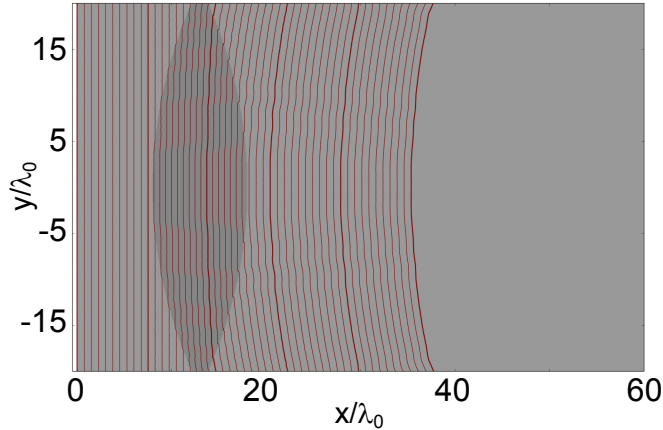


Figure 5: Wavefronts focused by a convergent lens of refractive index $N=1.2$.

Gaussian profile. Excellent results were obtained for a moderately focused Gaussian beam (Fig.6a), in good agreement with Gaussian optics theory (curves in Fig.6a) [45]. The geometrical optics solution is also shown and, as expected, is a good approximation away from the waist.

Fig.6 does not show wave intensities smaller than 10^{-8} , when normalized to intensities on the axis of the Gaussian beam. This corresponds to fractional electric fields of 10^{-4} . Similar criteria were adopted in truncating the very edge of the wavefront diffracting around the obstacle in Fig.2.

At even smaller fields, the zero-search can fail and misplace portions of the wavefront. Although this error originates in typically uninteresting low- E regions, it should be noted that each wavefront is determined by the previous one. Hence, imprecisely traced portions of a wavefront might cause portions of “later” wavefronts to also be misplaced, or distorted. The ultimate result is that these errors can eventually affect finite- E regions. This is typically not the case for moderately focused beams (Fig.6a), but can be the case for the strongly focused ones (Fig.6b), which will be the subject of future work. The issue could be solved by an improved, adaptive definition of the interval for zero-search by the bisection method. Additionally, here the zero search was performed for simplicity in the x direction (see search-intervals in Fig.4b). However, more customised search-intervals (orthogonal to the wavefront, or, better, parallel to group velocity) would aim at regions of high E and avoid low E and associated issues.

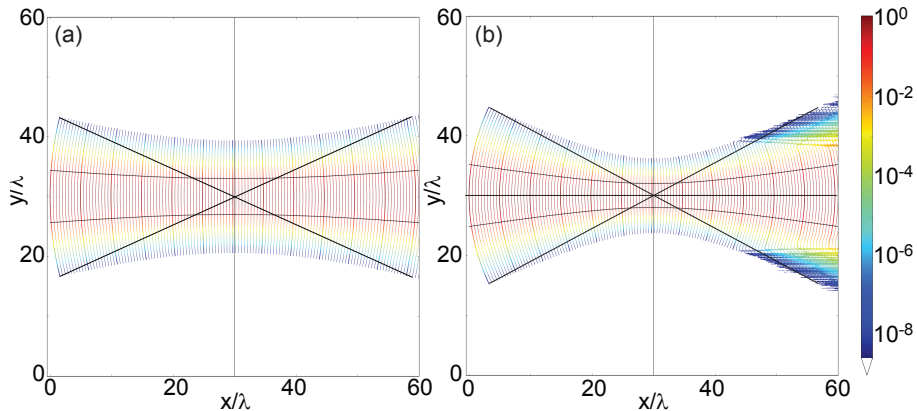


Figure 6: Wavefronts for (a) moderately and (b) strongly focused Gaussian beam, colored according to intensity normalized to on-axis value. One in every ten wavefronts is bold, as a guide for eyes. Also shown are the exact solutions for the contours at $1/e^2$ of central intensity (black curves on red background).

4. Discussion

By virtue of Fresnel's principle, the method naturally includes diffraction. This is an advantage over ray tracings and *truncated* paraxial expansions used in beam-tracings.

Another advantage of the method is that it only requires sub-wavelength resolution *along* the wavefront. *Across* the wavefront, however, the search for the next wavefront only requires a handful of points: if we assume the next wavefront to be one wavelength λ away from the current one, then only $\log_2 100$ iterations, -that is, 6 or 7- are needed to localize a point on the next wavefront with $\lambda/100$ accuracy. This is an important advantage over methods needing 100 points or elements per wavelength. Moreover, the next wavefront can be searched at more than a wavelength from the previous one, resulting in a further speed-up. This is possible because complete diffraction formulas are used here, instead of near-field approximations.

Going in more details, let us estimate the number of point-to-point calculations N_{ops} needed to trace N_{WT} wavefronts discretized by N_E points. Here by point-to-point we mean the contribution of a specific point emitter to a specific observation point (the argument of the sums in Eq.5). Localizing each point requires calculating the total field according to Eq.5 in N_{bis} trial-points. These are the points needed by the bisection method to converge to

a zero. In turn, each total field is calculated as the sum over a total of N_E emitters, in the worst case (i.e., on the net of truncations). Hence, a total of $N_{ops} = N_E^2 N_{WT} N_{bis}$ point-to-point calculations is needed.

Wavefront-spacing is not constrained by the wavelength, but needs to be much smaller than the non-uniformity length-scale normally to the wavefront, L_{\perp} . Nevertheless, it is reasonable to assume that wavefront-spacing is a fraction f of the wavelength. Therefore, $N_{WT} = N_{\lambda\perp}/f$, where $N_{\lambda\perp}$ is the number of wavelengths in the direction orthogonal to the wavefront. In that case, reaching the orthogonal precision of a full-wave solver deploying N_{ppw} points per unit wavelength imposes $N_{bis} = \log_2(f N_{ppw})$. In conclusion, $N_{ops} = N_E^2 N_{\lambda\perp} \log_2(f N_{ppw})/f$.

As mentioned in Sec.2.5, unequally spaced Fast Fourier Transform methods [44] could further speed up the method by replacing $N_E^2 \rightarrow N_E \log N_E$.

5. Future work

In the original Huygens-Fresnel integral, k was a fixed scalar, but *non-uniformity* is easily taken into account by letting $k = k(x)$, as done in Sec.2.

Also, the term in Huygens integrand assumed isotropy: k is a scalar, meaning that wavelets expand in all directions $\mathbf{x}' - \mathbf{x}$ with the same wavelength and same phase velocity ω/k .

In *anisotropic* media, however, global wavefronts as well as local wavelets expand at different velocities in different directions. Spherical wavelets are thus replaced by ellipsoids, elongated or compressed in the direction of anisotropy. Such ellipsoids do not preserve their aspect ratio, because some axes expand faster than others. It is easy to account for this by letting $k = k(\mathbf{x}, \mathbf{x}' - \mathbf{x})$. The wavenumber now depends on the line-of-sight $\mathbf{x}' - \mathbf{x}$ connecting the emitter with the observer (for example it depends on whether such direction is parallel, perpendicular or oblique to the direction of anisotropy). k is provided by the dispersion relation for the wave of interest, in the polarization (mode) of interest, and in the direction $\mathbf{x}' - \mathbf{x}$ of interest. An earlier treatment of anisotropy in terms of TE and TM modes [46] arrived to the same ellipsoidal wavelet representation.

Finally, further generalizing $\mathbf{k} = \mathbf{k}(\mathbf{x}, \mathbf{x}' - \mathbf{x}, mode)$ to be a complex, mode-dependent vector, not necessarily parallel to $\mathbf{x}' - \mathbf{x}$, accounts respectively for *absorption*, *birefringence* and *decoupling between phase and group velocity*. The phase velocity is parallel to \mathbf{k} , the group velocity describes

energy propagation from an array of points \mathbf{x} to an array of points \mathbf{x}' . Incidentally, phase and group velocity are decoupled also in ray tracings, allowing for non-parallel increments of ray position $d\mathbf{r}$ and of wavevector, $d\mathbf{k}$.

The underlying theory for $\mathbf{k} = \mathbf{k}(\mathbf{x}, \mathbf{x}', mode)$ (dispersion relation) is very well-established, but was never inserted in Huygens formulas.

Further improvements can be realized by modifying the integrand in Eqs.2-3 by way of special functions:

- Ref.[15] proposed to treat *caustics* by strategically ignoring some points of the old wavefront. In Ref.[33] it was proposed to address caustics by replacing with Airy functions the field radiated by point-sources.
- Bessel functions, on the other hand, can model the diffraction of *evanescent waves* in the near field [32].
- Airy and parabolic cylinder functions can replace oscillating fields in some evanescent *mode-conversion* regions [47].

Summary and Conclusions

We explored the applicability of the Huygens-Fresnel principle to a new method for wave propagation in non-uniform media.

Very briefly, the wavefront is discretized in an array of point-emitters of wavelets. A zero-search identifies observation points where the wavelets interfere destructively. Those zeros of field form an iso-phase surface, that is easily generalized to other phases. Then the process is repeated.

Some very simple cases were successfully modeled in 2D, including diffraction around an obstacle, refraction in slowly-varying and discontinuous media, Gaussian beams.

Minor issues of phase-jumps and corrugations were encountered, and fixed respectively by improved selection of zero-search intervals, and by adding “ghost cells” outside of the computational domain.

Future work was outlined and discussed, regarding extensions to anisotropic, birefringent, absorbing media such as magnetized plasmas.

Acknowledgements

The first author gratefully acknowledges fruitful discussions with R. Bilato, M. Brambilla, O. Maj and E. Poli, all at IPP Garching, Germany.

References

- [1] C. Huygens, *Traité de la Lumiere*, Leyden, 1690.
- [2] M. Born, E. Wolf, *Principles of Optics*, Cambridge University Press, 2006.
- [3] A. Fresnel, *Ann. Chem. Phys.* 1 (1816) 239.
- [4] A. Fresnel, *Mem. Acad.* 5 (1826) 339.
- [5] B. Baker, E. Copson, *The Mathematical Theory of Huygens' Principle*, AMS Chelsea Publishing, 1987.
- [6] M. Schwartz, *Principles of Electrodynamics*, Dover, Mineola, NY, 1987.
- [7] D. Miller, *Optics Lett.* 16 (1991) 1370.
- [8] P. Falstad, <http://www.falstad.com/ripple/> (2014).
- [9] W. Fendt, <http://www.walter-fendt.de/ph14e/huygenspr.htm> (2010).
- [10] C. Pfeiffer, A. Grbic, *Phys. Rev. Lett.* 110 (2013) 197401.
- [11] C. Lomnitz, Y. Meas, *Geophys. Res. Lett.* 31 (2004) L13613.
- [12] N. Rawlinson, J. Hauser, M. Sambridge, *Advances in Geophys.* 49 (2008) 203.
- [13] M. de Kool, N. Rawlinson, M. Sambridge, *Geophys. J. Int.* 167 (2006) 253.
- [14] F. Qin, Y. Luo, K. Olsen, W. Cai, G. Schuster, *Geophysics* 57 (1991) 478.
- [15] P. Sava, S. Formel, *SEP Report* 95 (1997) 101.
- [16] P. Sava, S. Formel, *Geophysics* 66 (2001) 883.
- [17] W. Hofer, *Proc. IEEE* 79 (1991) 1459.

- [18] L. Pierantoni, A. Massaro, T. Rozzi, A tlm node for the diffraction by 3d-dielectric corners based on the simultaneous transverse resonance method, in: IEEE MTT-S International Microwave Symposium digest. IEEE MTT-S International Microwave Symposium, 2005, pp. 1077–1080.
- [19] X. Jiao, *J. Comput. Phys.* 220 (2006) 612.
- [20] E. Agu, F. Hill, A simple method for ray tracing diffraction, in: Proc. ICCSA'03 Proceedings of the 2003 international conference on Computational science and its applications: PartIII, 2003, pp. 336–345.
- [21] S. Luo, J. Qian, R. Burridge, *J. Comput. Phys.* 270 (2014) 378.
- [22] P. Enders, *Eur. J. Phys.* 17 (1996) 226.
- [23] D. Luke, J. Burke, R. Lyon, *SIAM Rev.* 44 (2002) 169.
- [24] E. Tracy, A. Brizard, A. Kaufman, A. Richardson, *Ray Tracing and Beyond: Phase Space Methods in Plasma Wave Theory*, Cambridge Univ. Press, Cambridge, 2014.
- [25] D. Batchelor, R. Goldfinger, H. Weitzner, *IEEE Trans. Plasma Sci.* PS-8 (1980) 78.
- [26] F. Volpe, H. Laqua, *Rev. Sci. Instrum.* 74 (2003) 1409.
- [27] E. Poli, A. Peeters, G. Pereverzev, *Comp. Phys. Comm.* 136 (2001) 90.
- [28] N. Bertelli, O. Maj, E. Poli, R. Harvey, J. Wright, P. Bonoli, C. Phillips, A. Smirnov, E. Valeo, J. Wilson, *Phys. Plasmas* 19 (2012) 08510.
- [29] M. Brambilla, *Plasma Phys. Control. Fusion* 41 (1999) 1.
- [30] E. Jaeger, L. Berry, E. DAzevedo, et al., *Phys. Plasmas* 15 (2008) 072513.
- [31] V. Vdovin, *Fusion Science & Technology* 59 (2011) 690.
- [32] K. Makris, D. Psaltis, *Optics Communications* 284 (2011) 1686.
- [33] Y. Kravtsov, Z. Feizulin, *Radiophysics and Quantum Electronics* 12 (1969) 706.

- [34] P. Baues, *Opto-Electronics* 1 (1969) 37.
- [35] J. Monzon, *IEEE Trans. Microwave Theory Tech.* 41 (1993) 1995.
- [36] A. Ghatak, *Optics*, McGraw-Hill, 2009.
- [37] A. Gitin, *Applied Optics* 52 (2013) 7419.
- [38] P. Johns, *IEEE Trans. Microwave Theory Tech.* MTT-22 (1974) 209.
- [39] S. Nonogaki, *Japanese Journ. Appl. Phys.* 28 (1989) 786.
- [40] M. Al-Joumayly, N. Behdad, *IEEE Trans. Antennas Prop.* 58 (2010) 4033.
- [41] J. Tetienne, R. Blanchard, N. Yu, et al., *New Journal of Physics* 13 (2011) 053057.
- [42] K. Hammond, S. Massidda, W. Capecchi, F. Volpe, *J. Infrared Milli. Terahz Waves* 34 (2013) 437.
- [43] R. Burden, J. Faires, A. Burden, *Numerical Analysis*, Cengage Learning, 2015.
- [44] A. Dutt, V. Rokhlin, *SIAM J. Sci. Comput.* 14 (1993) 1368.
- [45] P. Goldsmith, *Quasioptical Systems*, Wiley, 1998.
- [46] L. Bergstein, T. Zachos, *Journ. Opt. Soc. America* 56 (1966) 931.
- [47] F. Volpe, *Phys. Lett. A* 374 (2010) 1736.